Proceedings of the 28th IEEE
EMBS Annual International Conference
New York City, USA, Aug 30-Sept 3, 2006

Current Source for Multifrequency Broadband Electrical Bioimpedance Spectroscopy Systems. A Novel Approach

Fernando Seoane, Ramon Bragós and Kaj Lindecrantz

Abstract— **New research and clinical applications of broadband electrical bioimpedance spectroscopy arise; increasing the upper limit frequency used in the measurement systems. The current source, an essential block of an electrical bioimpedance impedance analyzer, must have a large-enough output impedance at any frequency of operation to keep the output current constant regardless of the value of working load. In this paper a novel approach to increase the output impedance of a common voltage controlled current source is proposed. The circuit is analyzed, implemented and tested. The results, remarking the significant effect of the circuit parasitic capacitances, show a clear increment of the output impedance, but smaller than the originally expected.**

I. Introduction

Measurements of electrical bioimpedance is a well-established practice in medicine for monitoring of physiological variables *e.g. respiratory rate by impedance pneumography* [1], or tissue state *e.g. ischemia* [2], or for assessment on body composition *e.g. the BIA method* [3]. In the past years new studies of electrical bioimpedance performing measurements at relative high frequencies, higher than the traditional 50 kHz, have arisen; areas of application are *e.g.* skin cancer [4 & 5], tumours [6], meningitis [7], brain cellular edema [8 & 9].

The mentioned growth in wideband electrical bioimpedance applications has increased the upper limit of the measurements frequency band up to 1 MHz or above, demanding biomedical impedance instrumentation to appropriately operate at such high frequencies.

Along with the development of these new applications several researchers have investigated design and implementation of electronic instrumentation for impedance measurement systems [10] operating around and above 1 MHz. A very important analog subsystem in an impedance meter is the current source and several design and approaches have been studied and implemented *e.g.* Current Conveyors [11], floating-mirrored transconductance amplifiers [12], Howland topologies [13] etc. Most of those implementations operate very well at frequencies in the order of kHz but their performance, output impedance mainly, degrades near 1 MHz falling below the 100 kHz.

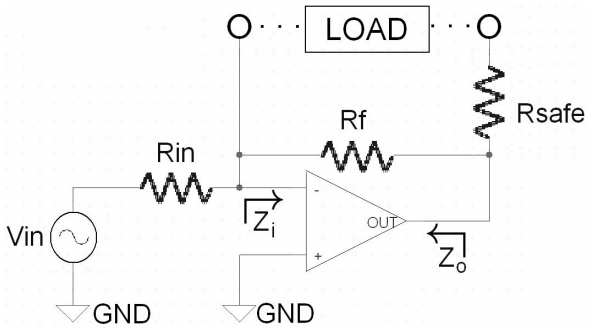

Fig.1. VCCS circuit based in a single Op-Amp in inverting configuration with the load in negative feedback

Recently we studied the performance of a Voltage Controlled Current Source (VCCS) based in a single-operational inverting topology [14], see Fig. 1. In the study

$$Z_{out} = R_{safe} + R_f \left\| \left(Z_o + \left(R_{in} \left\| Z_i \right. \right) \left(Ad + 1 \right) \left(1 - \frac{1}{2CMRR} \right) \right) \right. \quad (1)$$

$$Z_{in} = R_{in} \left\| Z_i \right. \quad (2)$$

we focused in the interdependencies between the circuit elements and the performance of the VCCS with particular attention on the output impedance, Z_{out}, expression in (1).

From (1) and (2) it is possible to appreciate the role of the equivalent input impedance, Z_{in}, of the VCCS in the Z_o of the overall current source. An increment in Z_i implies a proportionally direct increment in Z_{out} and with this idea in mind we have modified the single-operational based VCCS topology from Fig.1 replacing the Thevenized source *Vin* by a Norton source. In other words driving the circuit in Fig. 1 with current instead of voltage and therefore increasing R_{in} to R_{in} + Z_{out_I}, being Z_{out_I} the output impedance of the Norton source.

In this work, following an original approach, we propose and implement a novel design and test its performance with reference to the Z_{out}. The results are analysed and the observed limitations are discussed providing new and useful

Manuscript received April 24, 2006. This work was supported in part by the Swedish Research Council (research grant number 2002-5487), the European Commission (The BIOPATTERN Project, Contract No. 508803) and the *Karl G. Eliassons tilläggsfond*.

Fernando Seoane is with the School of Engineering at the University College of Borås, Borås, 50190, Sweden and the Division of Biomedical Engineering of the Department of Signals & Systems at Chalmers University of Technology, Gothenburg, SE 412 96, Sweden, (corresponding author, phone: +46334354414; fax: +46334354008; e-mail: fernando.seoane@hb.se).

Ramon Bragós is with the Department of Electronics at the Technical University of Catalonia, Barcelona, 08034 Spain. (e-mail: rbb@eel.upc.edu).

Kaj Lindecrantz is with the School of Engineering at the University College of Borås, Borås, 50190, Sweden (e-mail: kaj.lindecrantz@hb.se).

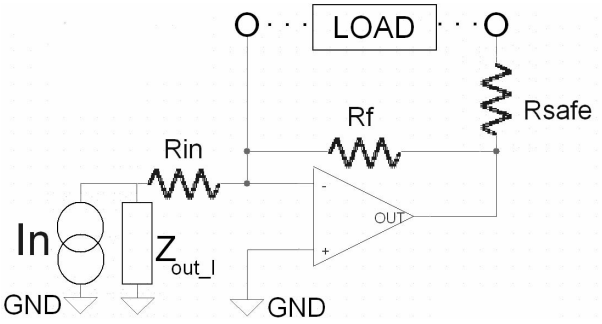

Fig. 2. Proposed design. A Current source based in a single Op-Amp circuit in inverting configuration driven by current. Note that the new R_{in} equivalent is R_{in} in series with Z_{out_I}.

information for the design of current sources for wideband electrical bioimpedance spectroscopy systems.

II. Methodology

A. Circuit Implementation

The proposed approach to drive the VCCS with current instead than voltage, see Fig.2, has been implemented using AD844 current conveyor as the Norton source and the LMH6655 as Op-Amp of the original VCCS circuit on an eurocard single-sided prototyping board.

B. Equivalent Model Analysis

The proposed circuit has been analyzed using the equivalent model of a non-ideal Op-Amp and the model of the current conveyor AD844, Fig. 3. The common-mode input impedance, $Z_{ic,}$ and the differential-mode input impedance, Z_{id}, have been calculated following [15] and using the values provided by the manufacturer in the datasheet. The gain of the operational, *G(f)*, is frequency dependent in the form $A_d(s)V_d(s)+A_{cm}(s)V_{cm}$, therefore the $CMRR(s)= A_d(s)/A_{cm}(s)$, it is also frequency dependent. The resulting expression for the equivalent Z_{in} and Z_{out} have been developed and theirs values have been calculated introducing the values of the discrete components and the integrated circuit specifications of the Op-Amps used in the implementation.

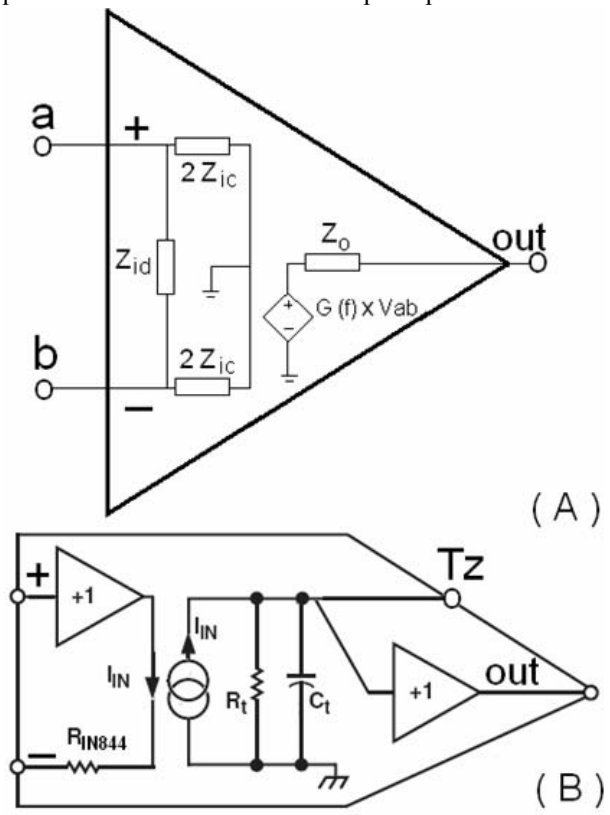

Fig. 3. Equivalent models. (A) Equivalent model of a non-ideal Operational Amplifier and (B) the equivalent model of the AD844 current conveyor.

C. Output Impedance Measurements

The output impedance of the current source has been measure using the impedance analyzer LCR HP4192A in Gain/Phase measurement mode following the technique used by Bertemes-Filho in [16].

III. Circuit Analysis

A. General Circuits Considerations

From (1) and (2) we can see that the output impedance of such VCCS depends mainly of the specifications of the Op-Amp integrated circuit, *Ad, CMRR and* Z_i, and the discrete external resistors, R_f *and* $R_{in,}$ used for its implementation. At low frequency the value of Z_{out} it is dominated by the resistor R_f with an approximate value of 400 kOhms and at high frequencies the dominating factor is the frequency dependent term $A_d(s)x\ Z_{in}$.

In order to increase the Z_{out} of the VCCS, after selecting the Op-Amp with the best set of specifications for the application, the next option is to deal with R_f and R_{in}.

Since in a bioimpedance application the input of the VCCS is uncoupled from DC through an uncoupling capacitor in series with R_{in}, as well as is the load by the electrodes, the only path for the bias current to ground is through R_f. Therefore in this case R_f cannot be remove and it can be increase only up to a certain value restricted by the bias current and the operation power supply of the Op-Amp.

$$I_{out} \simeq I_{in} = \frac{V_{in}}{R_{in}} \tag{3}$$

The role of R_{in} in this circuit is twofold; it contributes to

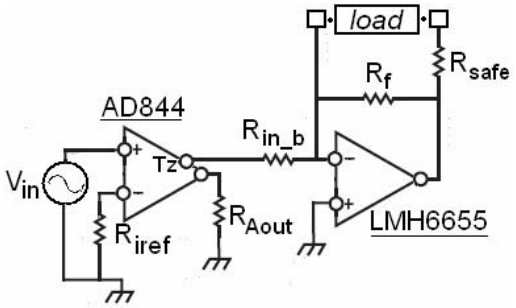

Fig. 4. The proposed current source. A single Op-Amp VCCS circuit driven by current conveyor

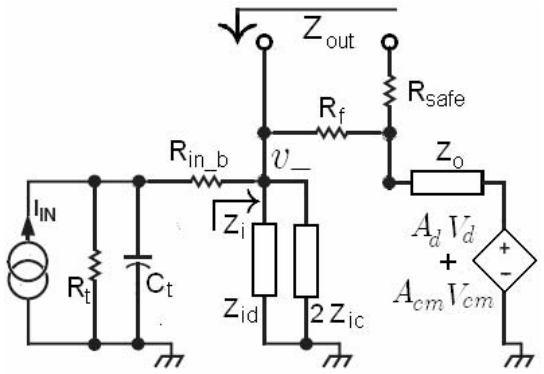

Fig. 5. Equivalent circuit model used to calculate the output impedance of the proposed current source in Fig.4.

the Z_{out} plus it also determines the input & output currents, see (3). Therefore due to such a relationship with the voltage at the input, V_{in}, and the current at the output, R_{in} cannot be increased freely. The way to be able to increase R_{in} with certain freedom is to remove the relationship in (3).

By driving the VCCS by current the output current will be totally independent from the value of R_{in}. The current will be generated by the current conveyor AD844 in a previous stage, see Fig.4. This way R_{in} can be increased considerably without affecting the output current. Regarding the equivalent circuit for the calculation of Z_{out} in Fig. 5, a new corresponding R_{in} is obtained, $R_{in} = R_{in\_b} + R_t \,\|\, C_t$.

B. New Current Source Specifications

1) Output current. The value of the output current in the current source circuit proposed in Fig. 4 is determined by the

$$I_{out} \simeq I_{in} = \frac{V_{in}}{R_{iref} + R_{IN844}} \tag{4}$$

relationship between V_{in} and R_{iref} at the input of the AD844 as defined in (4). This way the output current is generated independently from R_{in_b}, previous R_{in} in Fig.1.

2) Output impedance. The obtained expression for the output impedance in (5) is similar to the expression in (1) with the difference that the term R_{in} is now replace by the term $R_{in\_b} + R_t \,\|\, C_t$. In the original circuit the value of R_{in} set the value of the parallel connection Z_{in} in (2), typically the value of R_{in} is smaller than Z_i in the operation frequency range. In the proposed circuit this time the limiting term is the value of Z_i.

All the values used in the calculations and in the circuit implementation are found in Table 1. Z_{id} is the differential input impedance, $R_{id} \,\|\, C_{id}$, and Z_{ic} is the common mode input impedance, $R_{ic} \,\|\, C_{ic}$, of the LMH6655 Op-Amp circuit, see (6), while $R_t \,\|\, C_t$ is the output impedance of the terminal T_z of the AD844 current conveyor circuit. These values are extracted from the respective datasheets.

$$Z_{out} = R_{safe} + R_f \,\|\left(Z_o + \left(\left(R_{in\_b} + R_t \,\|\, C_t \right) \| \, Z_i \right) \left(Ad + 1 \right) \left(1 - \frac{1}{2CMRR} \right) \right) \tag{5}$$

$$Z_i = 2Z_{ic} \,\|\, Z_{id} \tag{6}$$

TABLE I
VALUES AND EXPRESSIONS FOR THE ELECTRICAL PARAMETERS

Symbol	Value/Expression	Frequency Dependency & Notes
R_f	390 kOhms	
R_{safe}	390 Ohms	
R_{in}	6.2 kOhms	
Z_o	0.08 Ohms	
R_{id}	20 kOhms	
C_{id}	0.55 pF	
R_{ic}	4 Mohms	
C_{ic}	0.9 pF	
R_{in_b}	6.2 kOhms	
R_t	3 MOhms	
C_t	4.5 pF	
C_{i_p}	10 pF	*parasitic*
C_{t_p}	10 pF	*parasitic*
C_{f_p}	0.25 pF	*parasitic*
$A_d(\omega)$	$A_{do} \Big/ \left(1 + \omega / \omega_0 \right)$	A_{d0} = 67dB $\omega_0 = 2\pi 125000$ rad x s^{-1}
$CMRR(\omega)$	$CMRR_o \Big/ \left(1 + \omega / \omega_0 \right)$	$CMRR_0$ = 90dB $\omega_0 = 2\pi 9000$ rad x s^{-1}

Only values related to Z_{out} and Z_{in}.

IV. RESULTS

In Fig. 6 it is possible to see from the calculated Z_{out}, the effect of driving the original VCCS with currents instead than voltage. The calculated Z_{out} of the circuit, continuous trace, in Fig. 4 is larger than the Z_{out} of the original circuit, discontinuous trace, However the expected and calculated large increment it is not shown in the experimental measurements, also in Fig. 6. At the frequency of interest, 1 MHz, the measured Z_{out} of the proposed circuit, filled-dot trace, is slightly larger than the Z_{out} of the original VCCS, hollow-dot trace.

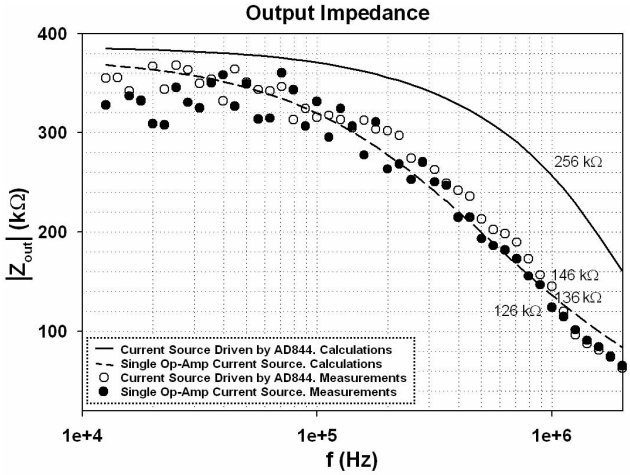

Fig. 6. Plots of the output impedance, measurements and calculations, for each of the circuits.

Fig. 7 contains the measured Z_{out} for each of the circuits and the calculated Z_{out}, this time including the effect of parasitic capacitances. C_{i_p} is the parasitic capacitance associated in parallel to the input of the LMH6655, C_{t_p} is

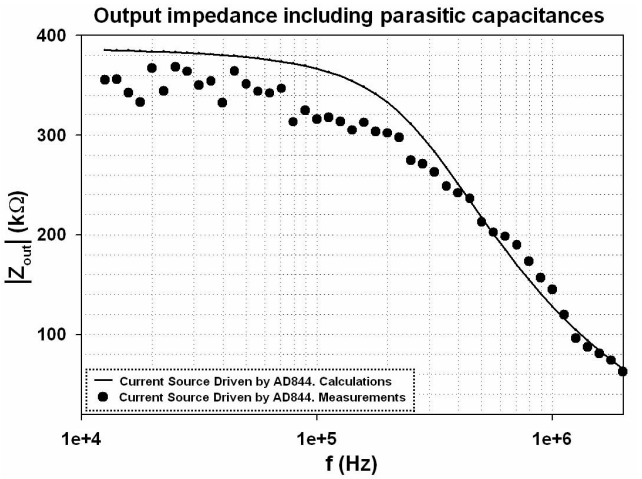

Fig. 7. Plots of the output impedance, measurements and calculations, for proposed circuit, including parasitic capacitances.

associated to the output of the AD844 and C_{f_p} is associated to the output of the VCCS in parallel with R_f. As it is possible to observe in the figure the plots, especially at high frequencies, fit relatively well. Therefore at the frequency of interest, around 1 MHz and above, the Z_{out} is highly influenced by the parasitic capacitances.

V. Discussion

Studying the Z_{out} resulting from the calculations we could say that the initial approach of increasing Z_{in} in (2) to enlarge the overall Z_{out} was valid up to certain extend; The Op-Amp impedance factor *opz* is derivate from (1) and defined in (7) as:

this factor is the total contribution of the Op-Amp to the overall output impedance of the current source and its influence it is a key element. The role the *opz* factor in the total output impedance is to enlarge the contribution of the input resistance and attenuate the effect of the capacitances at the input. See Figure 8. As the *opz* factor is frequency dependent and its value decrease with increasing frequency the enlargement and attenuation effects decrease as well.

At frequencies of 1 MHz and above, the effect of the circuit and parasitic capacitances, otherwise negligible, is determinant. In this case, connecting the T_z output of the AD844 at the input of the VCCS has introduced a new parasitic capacitance. This capacitance contributes to the already present input capacitance at the inversor input of the Op-Amp partially canceling the increasing input impedance effect obtained by introducing the current conveyor. This resulting input capacitance, approximately >90% parasitic, attenuated by the factor *opz*, is the main contributor to the output capacitance of the current source; it is like propagated to the output, see Fig. 8.

Probably with a careful circuit implementation, *i.e.* use of only SMD components, short connections, avoid parallel tracks, etc, the effect of the parasitic capacitance could be minimized significantly and as a consequence allowing

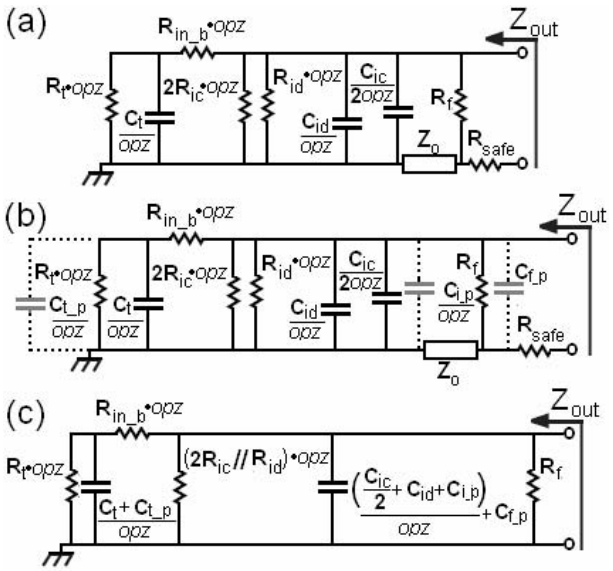

Fig. 8. Equivalent circuits for the output impedance of the proposed current source circuit. In (a) the equivalent circuit of the ideal VCCS, in (b) including parasitic capacitances, indicated with a discontinuous trace, and (c) a simplified circuit equivalent. **N.B.** R_{safe} and Z_o are very small and can be neglected.

output impedances in the range of 200 KOhms over 1 MHz.

The limiting effect of the output capacitance, circuit intrinsic and parasitic, on the output impedance of current

$$opz = (Ad+1)\left(1-\frac{1}{2CMRR}\right) \quad (7)$$

sources has been studied for sometime and there is a method able to cancel this capacitance; the use of Generalized Impedance Converters (GICs) or Negative Impedance Converters (NICs) to generate an inductance able to compensate the value of the output capacitance.

This way, it is possible to achieve spectacularly high values for Z_{out} [18], but only at a single selectable frequency. This solution is not very efficient for multifrequency measurements systems. GICs & NICs must be trimmed for a specific frequency at the time, therefore needing a large number of adjustable and switchable components. Consequently, it is suitable only for frequency sweeping systems and not for multisine systems. On top of that using GIC & NICs increases the instability of the current source.

Regarding the output current, with the proposed circuit the value of the current is basically set by the relationship between the Voltage at the input V_{in} and the value of R_{iref}, the resistor at the inverting input of the current conveyor. **N.B.** The value of R_{IN844} is very small and can be neglected. See (4). This way, the value of the output current is completely independent of any parameter related to the output specifications and that is always and advantage in a current source.

VI. Conclusion

As we have shown here and in [14], it is possible to design efficient and practical current sources circuits with large enough output impedances for multifrequency broadband electrical bioimpedance, above 100 kOhms at 1 MHz.

The developments in electronic design in the past years have made available wide-bandwidth Op-Amps that allow us the use of basic structures, like the implemented here, to obtain a current source with good performance at high frequencies without the need of making use of complex structures.

A key factor to obtain a current source with high output impedance is to relate the features of the current-source with the Op-Amp parameters in order to select the correct device. An appropriate Op-Amp circuit is one with the following specifications: high input impedance, low bias current and differential gain with the first pole in the frequency range of hundreds of KHz. However in order to truly make use of the good specifications of any wideband Op-Amp at such high frequencies, the main obstacle to overcome is no the circuit design as such, if not to deal with the always-present parasitic capacitances.

VII. Acknowledgements

The authors would like to thank Ph.D. Ants Silberberg and Roger Malmberg for their helpful comments on the performance of Op-Amp Circuits and the effect of parasitic capacitances.

References

[1] T. Olsson, L. Victorin, "Transthoracic impedance, with special reference to newborn infants and the ratio air-to-fluid in the lungs," *Acta Paediatr. Scand.*, vol. 207, Suppl. 1+, 1970.

[2] M. Genesca *et al*, "Electrical bioimpedance measurement during hypothermic rat kidney preservation for assessing ischemic injury," *Biosens. Bioelectron.*, Vol.15, no.20, is. 9, pp. 1866-1871, Mar. 2005.

[3] R.F. Kushner, "Bioelectrical impedance analysis: a review of principles and applications," *J Am. Col.l Nutr*., vol. 2, no. 11, pp. 199-209, April1992.

[4] P. Åberg, *et al*, "Skin cancer identification using multifrequency electrical impedance—a potential screening tool," *IEEE Trans. Biomed. Eng.,* vol. 51, no. 12, pp. 2091–2102, Dec. 2004.

[5] D. G. Beetner, S. Kapoor, S. Manjunath, X. Zhou and W. V. Stoecker, "Differentiation among basal cell carcinoma, benign lesions, and normal skin using electric impedance," *IEEE Trans. Biomed. Eng.,* vol. 50,no. 8 pp. 1020–1025, Dec. 2004.

[6] C. Skourou, P. J. Hoopes, R. R. Strawbridge and K. D. Paulsen "Feasibility studies of electrical impedance spectroscopy for early tumor detection in rats," *Physiol. Meas.*, vol. 25, pp. 335–346, 2004.

[7] B. K. van Kreel, "Multi-frequency bioimpedance measurements of children in intensive care, *Med. Biol. Eng. Comput.*, vol. 39, pp. 551–557, 2001.

[8] B.E. Lingwood, K.R. Dunster, G.N.Healy, L.C. Ward and P.B. Colditz. "Cerebral impedance and neurological outcome following a mild or severe hypoxic/ischemic episode in neonatal piglets," *Brain Research*, vol. 969, pp. 160 – 167, 2003.

[9] F. Seoane, *et al*, "Spectroscopy study of the dynamics of the transencephalic electrical impedance in the perinatal brain during hypoxia". Physiol. Meas., vol. 26, pp. 849-863, Oct.2005

[10] K. G. Boone and D. S. Holder, "Current approaches to analogue instrumentation design in electrical impedance tomography," *Physiol. Meas.*, vol. 17**,** pp. 229–247, 1996.

[11] R. Bragós, J. Rosell and P.J. Riu, "A wideband AC-coupled current for electrical impedance tomography," *Physiol. Meas.*, vol. 15**,** pp. A91–A99, 1994.

[12] J. J. Ackmann, "Complex bioelectric impedance measurement system for the frequency range from 5 Hz to 1Mhz," *Ann. Biomed. Eng*., vol. 21, pp. 135-146, 2003

[13] J. Jossinet, C. Tourtel and R. Jarry, "Active current electrodes for in-vivo electrical impedance tomography," *Physiol. Meas.* Vol. 15, Suppl. 2A, pp. 83–90, 1994.

[14] F. Seoane, R. Bragós and K. Lindecrantz, "Current source for wideband electrical bioimpedance spectroscopy Based on a single operational amplifier," submitted to the World Congress on Medical Physics and Biomedical Engineering 2006.

[15] R.C. Jaeger and T.N. Blalock, *Microelectronic Circuit Design, 2nd Ed*. Singapore: McGrw Hill, 2004, ch. 11, p.752.

[16] P. Bertemes-Filho, B. H. Brown and A. J. Wilson, "A comparison of modified Howland circuits as current generators with current mirror type circuits," *Physiol. Meas.* Vol. 21, pp. 1–6, 2000.

[17] A. S. Ross, G. J. Saulnier, J. C. Newell and D. Isaacson, "Current source design for electrical impedance tomography," *Physiol. Meas.* vol. 24 pp. 509–516, 2003.